

1 **Brief Research Report**

Peptidome profiling for the immunological stratification in sepsis: a proof of concept study

2 **Martín Ledesma^{1, 7}, María Florencia Todero², Lautaro Maceira², Monica Prieto³, Carlos**
3 **Vay¹, Marcelo Galas⁴, Beatriz López⁵, Noemí Yokobori^{6, 7}, Bárbara Rearte^{2, 7*}**

4 ¹ Laboratorio de Bacteriología, Departamento de Bioquímica Clínica, Hospital de Clínicas “José de
5 San Martín”; Facultad de Farmacia y Bioquímica, UBA, Buenos Aires, Argentina.

6 ² Instituto de Medicina Experimental (IMEX) - CONICET - Academia Nacional de Medicina, Buenos
7 Aires, Argentina.

8 ³ Servicio de Bacteriología Especial. Instituto Nacional de Enfermedades Infecciosas (INEI), ANLIS
9 “Dr. C. G. Malbrán”, Buenos Aires, Argentina.

10 ⁴ Special Program of AMR, Communicable Diseases and Environmental Determinants of Health
11 Department, Pan-American Health Organization, Washington, D.C., USA.

12 ⁵ Departamento de Bacteriología. INEI, ANLIS “Dr. C. G. Malbrán”, Buenos Aires, Argentina.

13 ⁶ Servicio de Micobacterias INEI, ANLIS “Dr. C. G. Malbrán” Buenos Aires, Argentina.

14 ⁷ Consejo Nacional de Investigaciones Científicas y Técnicas (CONICET), Argentina.

15

16 *** Correspondence:**

17 Rearte Bárbara PhD.

18 barbararearte@yahoo.com.ar; barbararearte@gmail.com

19 **Keywords: Lipopolysaccharide, plasma, sepsis, Mass Spectrometry, Matrix-Assisted Laser**
20 **Desorption-Ionization, peptidome.**

21

22

23 **Abstract**

24 Sepsis has been called “the graveyard of pharmaceutical companies” due to the numerous failed
25 clinical trials. The lack of tools to monitor the immunological status in sepsis constrains the
26 development of immunomodulatory therapies. Here, we evaluated a test based on whole plasma
27 peptidome acquired in a MALDI-TOF-mass spectrometer used for bacterial biotyping and machine-
28 learning algorithms to discriminate the different immunological phases of sepsis. In this proof of
29 concept study, two discrete lipopolysaccharide-(LPS) induced murine models emulating the pro- and
30 anti-inflammatory phases that occur during sepsis were evaluated. The LPS group was inoculated
31 with a single high dose of LPS, recalling the proinflammatory phase, and the IS groups was subjected
32 to increasing doses of LPS to induce the anti-inflammatory/immunosuppression phase. Unstimulated
33 mice served as controls. Both experimental groups showed the hallmarks of pro- and anti-
34 inflammatory phases respectively; the LPS group showed leukopenia and higher levels of cytokines
35 and tissue damage markers, and the IS group showed neutrophilia, lymphopenia and significantly
36 lower antibody titers upon immunization. Principal component analysis of the plasma peptidomes
37 formed three discrete clusters that mostly coincided with the experimental groups. In addition,
38 machine-learning algorithms discriminated the different experimental groups with a sensitivity and
39 specificity of up to 95.7% and 90.9% respectively. Our data reveal the potential of plasma peptidome
40 analysis by MALDI-TOF-mass spectrometry as a simple, speedy and readily transferrable method for
41 sepsis patient stratification that would contribute to therapeutic decision-making based on their
42 immunological status.

43 1 Introduction

44 Sepsis constitutes one the major causes of death in intensive care units (Vincent et al., 2009; Novosad
45 et al., 2016) with an incidence of 31.5 million cases and 7-9 million deaths annually (Fleischmann et
46 al., 2016). The impact of sepsis in developing regions such as Latin America is elusive due to the
47 limited number of prevalence studies, but the high incidence rate of infectious diseases and the
48 inequities in the access to health care indicates that sepsis is an alarming health problem in the region
49 (Machado et al., 2017; Azevedo et al., 2018; Estenssoro et al., 2018; Estenssoro et al., 2019).

50 The redefinition by the Sepsis-3 consensus highlights the need to integrate the information on the
51 etiological agent and the host response status and strongly emphasizes that the dysregulated host
52 response as a key component of sepsis (Singer et al., 2016).

53 From the immunological point of view, sepsis is characterized by the predominance of an
54 overwhelming pro-inflammatory response during the early stages with a concomitant anti-
55 inflammatory and immunosuppressive response that becomes predominant in the later stages (van der
56 Poll et al., 2017; Venet et al., 2018; Rubio et al., 2019). Sepsis has earned the epithet of “the
57 graveyard of pharmaceutical companies” due to the numerous failed clinical trials and this could be
58 related to an inappropriate timing for the application of immunomodulatory interventions (Rubio et
59 al., 2019). The lack of tools to monitor the host immune status constrains the evaluation of novel
60 immunomodulatory therapeutic approaches. Despite the efforts put in biomarker search in the past
61 decades, only a handful of molecules, such as procalcitonin, proved to be useful in the clinical setting
62 under specific conditions, and the fact that efficient biomarkers not necessarily correspond to key
63 mediators adds further complexity (Parlato and Cavaillon, 2015). Moreover, none of them determines
64 the quickly changing immunological status of the host (Pierrakos and Vincent, 2010; van der Poll et
65 al., 2017; Parlato et al., 2018; van Engelen et al., 2018b; Venet et al., 2018; Al Jalbout et al., 2019;
66 Gunsolus et al., 2019; Rubio et al., 2019; Schenz et al., 2019).

67 With the advent of artificial intelligence algorithms including machine learning (ML) (López
68 Fernández et al., 2016), top-down analysis of unlabeled biological samples is gaining ground. This is
69 the case of matrix-assisted light desorption ionization-time of flight-mass spectrometry (MALDI-
70 TOF-MS), a powerful tool that is currently spreading in the clinical setting for microbiological
71 biotyping and in biomedical research for the study of biological samples in several diseases including
72 sepsis (Ludwig and Hummon, 2017; Hou et al., 2019).

73 Taking into account that around 50% of all sepsis cases are caused by Gram-negative bacteria (van
74 Engelen et al., 2018a; Dolin et al., 2019), we (Rearte et al., 2010a; Rearte et al., 2010b; Landoni et
75 al., 2012; Martire-Greco et al., 2014; Rearte et al., 2014; Córdoba-Moreno et al., 2019; Montagna et
76 al., 2020) and other authors (Opal et al., 1999; Genga et al., 2018) demonstrated that both
77 inflammatory and anti-inflammatory processes that occur during sepsis can be emulated by
78 lipopolysaccharides (LPS) in murine models.

79 Herein, we hypothesized that the pro/anti-inflammatory phases could be discriminated through the
80 analysis of plasma peptidome spectra generated by MALDI-TOF-MS. Thus, in this study, using LPS-
81 induced murine models emulating the different phases, we developed and evaluated predictive
82 models based on ML algorithm that would allow the discrimination of the different immunological
83 phases.

84 2 Materials and methods

85 2.1 Animals

86 Female and male BALB/c mice (8–12 weeks old) were provided by the IMEX-CONICET-Academia
87 Nacional de Medicina, Buenos Aires, Argentina. Animals were maintained under a 12 h light–dark
88 cycle at 22 ± 2 °C and were fed with standard diet and water *ad libitum*. Animals were bred and
89 housed in accordance with the NIH Guide and Use of Laboratory Animals (National Research
90 Council (U.S.), 2011). Experimental designs were approved by the Committee for the Care and Use
91 of Laboratory Animals (CICUAL) of IMEX-CONICET, Academia Nacional de Medicina de Buenos
92 Aires.

93 2.2 Murine Models

94 All the inoculation and sample collection schemes are depicted in Supplementary Figure 1.

95 Briefly, for the inflammatory phase model (LPS group), BALB/c mice were inoculated with a lethal
96 dose 50 (LD50) of LPS of *Escherichia coli* O111: B4 (100 µg/ mouse; Sigma-Aldrich, St Louis, MO,
97 USA) intraperitoneally (i. p.) (Córdoba-Moreno et al., 2019). Plasma samples were obtained at 1.5 h
98 and 6 h after the injection. In the anti-inflammatory/immunosuppression phase model (IS group),
99 BALB/c mice were inoculated daily with LPS for 10 consecutive days. The inoculation scheme
100 consisted of increasing doses starting from 5 µg/mouse i. p. for the first 4 days, followed by 50
101 µg/mouse i. p. for 3 days, and 100 µg/mouse i. p. for the last 3 days (Rearte et al., 2010b). Plasma
102 samples were obtained 24h after the last LPS dose. A third group of mice inoculated with vehicle
103 (saline solution) served as control (CTL group). The plasma in this group was collected at the same
104 time points indicated in the experimental groups. Peripheral blood was collected by submandibular
105 bleeding method in order to maximize the quality of the sample. Part of the heparinized samples were
106 used for blood cell count and the remaining volume was centrifuged twice (400xg, 10 min at 4°C)
107 and plasma were stored at -20°C until analysis.

108 2.3 Immunological, hematological and biochemical parameters

109 Peripheral blood leukocytes were counted in a Coulter hematology analyzer (Diatron Abacus Junior
110 Vet, Budapest, Hungary) at 1.5 h and 24 h post LPS for the LPS and the IS groups respectively.
111 Proinflammatory (TNF- α ; IL-12p70; IFN- γ ; IL-6) and anti-inflammatory cytokines (IL-10, TGF- β)
112 were determined in plasma by ELISA at the indicated time points (OptEIA set; BD Biosciences, San
113 Diego, CA, USA) according to the manufacturer's instructions. The tissue damage markers creatinine
114 (Cre), alanine aminotransferase (ALT) and aspartate transaminase (AST) were determined in plasma,
115 at 6 and 24 h in the LPS and IS groups respectively, using a kit from BioTecnica (Varginha, Minas
116 Gerais, Brazil) and the MINDRAY BS-200E auto-analyzer according to the manufacturer's
117 instructions.

118 For flow cytometry analysis, 24 h after the last LPS dose, a splenocyte suspension was obtained and
119 the cells were immunolabeled as described previously (Rearte et al., 2010b; Rearte et al., 2014). The
120 following cell types were evaluated: CD4 (FITC-anti-CD4, clone RM4-5) and CD8 (PECy5-anti-
121 CD8, clone 53-6.7) T-lymphocytes, B-lymphocytes (FITC-anti-CD45R-B220, clone RA3-6B2),
122 polymorphonuclear neutrophils (FITC-anti-CD11b, clone M1/70 and PE-anti-Ly6G, clone 1A8). The
123 expression levels of PDL-1 (PE-anti-PDL-1, clone MIH5) on the CD11b gate of myeloid lineage
124 cells were also evaluated. Labeled monoclonal antibodies were obtained from Invitrogen and BD
125 Pharmingen™. Cells were acquired in a Becton Dickinson FACScan flow cytometer using Cell
126 Quest software (Becton Dickinson, San Jose, CA, USA).

127 Primary antibody response to sheep red blood cells (SRBC) was evaluated by immunizing animals 24
128 h after the last dose of LPS (5×10^8 SRBC /mouse, 0.1ml i. p.). The anti-SRBC antibody titer was
129 evaluated in serum through an hemagglutination assay 7 days after immunization as described
130 previously (Rearte et al., 2010b; Rearte et al., 2014).

131 **2.4 Acquisition of MALI-TOF-MS spectra**

132 Plasma samples were analyzed with the MALDI Biotyper System (Bruker Daltonik GmbH, Bremen,
133 Germany). Total number of plasma samples analyzed per group were $n = 29$ for the LPS group, $n =$
134 22 for the IS group and $n = 25$ for the CTL group. Plasma samples were analyzed with the standard
135 method for microbial biotyping. Briefly, $1 \mu\text{l}$ of plasma was loaded onto each spot in duplicate and 1
136 μl of the matrix (alpha-cyano-4-hydroxycinnamic acid matrix in 50% acetonitrile and 2.5%
137 trifluoroacetic acid) was added to each dried spot.

138 Continuous mass spectra were obtained with a Microflex LT/SH MALDI-TOF mass spectrometer
139 using the flexControl software version 3.4.135.0. Acquisition conditions were ionization mode: LD+,
140 acquisition method: MBT_FC.par, acquisition mode: qsim, tof Mode: linear, acquisition Operator
141 Mode: linear, and digitizerType: Bruker BD0G5, within a mass range of 2,000-20,000 Da. Spectra
142 were obtained in the manual mode, using 60% of laser intensity with 40 laser repetition in each shot
143 and reaching between 400-500 spectra by acquisition. Internal calibration was performed every day
144 following manufacturer's instructions (bacterial test standard; Bruker Daltonik GmbH).

145 **2.5 MALDI-TOF-MS data pre-processing**

146 We generated a dataset containing 152 mass spectra from plasma samples corresponding to the three
147 mice groups in duplicate. Mass spectra were read as fid/aqus files with MALDIquantForeign (v0.10)
148 (Gibb, 2019) and they were processed using MALDIquant (v1.16.2) (Gibb and Strimmer, 2012) R
149 package. Briefly, spectra were square root-transformed, smoothed using the Savitzky-Golay
150 algorithm, and were baseline-corrected applying the SNIP process across 100 iterations.

151 The peaks were detected by a function that estimates the noise of mass spectrometry data by
152 calculating the median absolute deviation (MAD). The signal-to-noise-ratio (SNR) was set up in 4,
153 with a half Window Size of 40 and a tolerance of 0.2 for peak binning. Duplicates were averaged
154 except from one replicate corresponding to the CTL group that was removed due to low quality and
155 76 averaged spectra were subject to further analysis. Peaks that occurred in less than 33% of the
156 spectra were removed. MALDI-TOF-MS data were transformed by a categorization of the peak
157 intensity, performed with the Binda R package (Gibb, 2015) which compares the intensity value with
158 the peak group average, returning 1 when it was equal or higher and 0 when it was lower. The
159 analysis workflow is depicted in the Figure 1.

160 **2.6 Statistical analysis**

161 **2.6.1 Immunological, hematological and biochemical parameters**

162 Graph Pad Prism 6 software (GraphPad Software, San Diego, CA) was used for statistical analysis
163 and plotting. The number of mice or biological replicates (n) analyzed in each experiment were the
164 replicates considered for statistical analysis. Values are expressed as the mean \pm standard error of the
165 mean (SEM) of n samples. No outliers were removed. The assumption test to determine the Gaussian
166 distribution was performed by the Kolmogorov and Smirnov method. For parameters with a Gaussian
167 distribution, the differences between two experimental groups were assessed by unpaired Student's t
168 test, and for multiple group comparisons, as the differences in peripheral blood leukocytes, were

169 analyzed using a one-way ANOVA followed by a Tukey's multiple comparison test. For parameters
170 with a non-Gaussian distribution, comparisons between two experimental groups were performed
171 using Mann–Whitney U test. All statistical tests were interpreted in a two-tailed fashion and a $P < 0.05$
172 was considered statistically significant.

173 **2.6.2 MALDI-TOF-MS data**

174 Statistical analysis and plotting were performed using Rstudio. Programmed peaks selection was
175 performed in the entire dataset seeking for biomarkers of each class representing the different
176 experimental groups by the Binary Discriminant Analysis (BDA) algorithm, which outputs the
177 t.score (Class means vs. Pooled mean) of each peak. The sign of the t.score indicates the presence
178 (positive t.score) or absence (negative t.score) of that peak in each group. A significance level of 95%
179 was achieved if the modulus of the t.score was equal or higher than 2.5. The best-extracted features
180 were then used to perform a hierarchical k-means clustering-principal component analysis (PCA)
181 with the factoextra R package (Kassambara and Mundt, 2019). The binary distance was used to
182 measure dissimilarity between observations by the ward.D2 agglomeration method with a k of 4. In
183 addition, spectra were analyzed with the random forest (RF) classifier to test another classification
184 model based on a different underlying criterion.

185 Afterwards, two ML methods were applied in the dataset to train both BDA and RF classifiers in R
186 (Liaw and Wiener, 2002). Initially, the dataset was randomly partitioned into a training set (60% of
187 plasma samples) and a test set (40% of plasma samples). Programmed feature (peaks) selection was
188 performed with the respective algorithms in the training set seeking for discriminant peaks
189 corresponding to each experimental group. The extracted features were then used to train several ML
190 models. Accuracy, sensitivity, and specificity were used to evaluate the performances of all resulting
191 models in the test set by a cross-validation strategy.

192 **3 Results**

193 **3.1 Simulation of pro- and anti-inflammatory sepsis phases**

194 The proinflammatory phase was induced with a high dose of LPS (LPS group), whereas the anti-
195 inflammatory/immunosuppression phase (IS group) was reached with a scheme of increasing doses
196 of LPS (Suppl. Fig.1). In order to validate the two models, immunological, inflammatory and tissue
197 damage markers were studied in the two experimental groups as well as in the control group (CTL
198 group). In accordance with our previous results, the LPS group was characterized by a marked
199 leukopenia (Suppl. Fig 2a), high plasma levels of pro-inflammatory cytokines such as TNF- α but also
200 of the anti-inflammatory cytokines IL-10 and TGF- β (Suppl. Fig 3a, b). Tissue enzymes indicative of
201 damage were also elevated (Suppl. Fig 4a-c).

202 On the other hand, the IS group showed a leucocytosis due to increased numbers of circulating
203 granulocytes, particularly of polymorphonuclear neutrophils (Suppl. Fig 2b) (Córdoba-Moreno et al.,
204 2019), along with high plasma levels of TGF- β and low levels of pro-inflammatory cytokines
205 (Suppl. Fig 3c). No signs of tissue damage were observed in this group (Suppl. Fig 4d-f). As
206 previously described (Rearte et al., 2010b; Rearte et al., 2014; Montagna et al., 2020), IS mice had a
207 profound immunological impairment, accompanied by a marked lymphopenia and an increased
208 number of neutrophils in the spleen, which expressed higher levels of the inhibitory receptor PDL-1
209 (Suppl. Fig 5a, 5b). Moreover, the IS group showed significantly lower antibody titers upon
210 immunization with SRBCs (Suppl. Fig 5c). Collectively, these results indicate that the pro- and anti-
211 inflammatory/immunosuppression phases were emulated in our murine models.

212 3.2 MALDI-TOF MS data analysis

213 Plasma samples of the CTL, IS and LPS groups were analyzed by MALDI-TOF MS in the 2000 –
214 20,000 Da range. Representative spectra of each experimental group are shown in Suppl. Fig. 6 and
215 the analysis pipeline is detailed in Figure 1. A statistical analysis set was implemented to test if
216 MALDI-TOF MS data were useful to discriminate the three experimental groups. First, through a
217 supervised classification algorithm we looked for peaks that best differentiated the CTL, LPS, and IS
218 groups. The 20 best discriminant peaks identified by binary discriminant analysis (BDA) and random
219 forest (RF) algorithms are shown in the Suppl. Fig. 7a and b respectively, which partially overlapped.
220 Of the 20 best peaks selected by the BDA algorithm, the 10 most discriminant peaks were chosen for
221 an unsupervised statistical analysis to plot the hierarchical k-means clustering-PCA clusters (Figure
222 2a). Clusters appeared as three non-superimposed groups, and the first two principal components
223 explained 76.6% of the variation with good intra cluster homogeneity. Specifically, cluster 2
224 achieved 100% (16/16) of homogeneity for spectra corresponding to CTL plasma and 64% (16/25) of
225 CTL spectra fell in this cluster, while for cluster 1 an 85% (29/34) homogeneity was achieved for
226 spectra corresponding to the LPS group and 100% (29/29) of LPS spectra fell in this cluster (Figure
227 2b). Lastly, homogeneity of cluster 3 was 77% (20/26) mostly represented by spectra of the IS group,
228 with 91% of the IS spectra (20/22) included in this cluster. This result shows that the
229 immunosuppression/anti-inflammatory and pro-inflammatory phases have distinctive plasma
230 peptidome signatures that allow their discrimination.

231 3.3 Machine learning analysis

232 ML algorithms were used to develop a predictive model based on the plasma fingerprints, using a
233 training data set (14 CTL, 13 IS and 15 LPS samples) challenged with a test data set (11 CTL, 9 IS
234 and 14 LPS samples; Figure 1). To find the most refined model, a dimensionality reduction was
235 performed through the selection of different numbers of distinctive peaks in the training set to train
236 the algorithms, and the performances on the test set were computed for each condition. Specifically,
237 the top 5, 10, 15, and 20 discriminant peaks for BDA and RF algorithms were evaluated by cross-
238 validation (CV; 5 folds and 20 repetitions) and percentages of accuracy, sensitivity, specificity,
239 negative predictive value (NPV) and positive predictive value (PPV) in the test data set were
240 obtained (Table 1).

241 Between models, RF using the best 20 peaks showed the most consistent values, with sensitivity and
242 specificity values above 90%. The BDA model trained with the best five peaks showed the best
243 performance in terms of detection of positive cases, with a sensitivity above 95% (Table 1); this
244 strategy constitutes the simplest method in terms of both the number of required peaks and
245 computational demands. These results display the potential of plasma peptidome fingerprints to
246 develop predictive models.

247

248 4 Discussion

249 Sepsis constitutes a highly heterogeneous syndrome of complex pathophysiology. The underlying
250 immunological alterations that include pro-inflammatory, anti-inflammatory and immunosuppressive
251 components (Rubio et al., 2019) are reflected in septic plasma protein composition and varies over
252 time according to the disease severity (Hayashi et al., 2019).

253 In the last decades, several circulating markers with recognized functions in sepsis were identified.
254 However, none of these markers showed the specificity and sensitivity required for its clinical use
255 (Parlato et al., 2018; van Engelen et al., 2018b). Furthermore, methods that rely on immunolabeling
256 such as ELISA or flow cytometry, are highly specific and sensitive for the detection of low
257 abundance markers, but requires costly equipment and consumables, as well as specific technical
258 knowhow. In addition, these techniques are time consuming, limiting their clinical usefulness for
259 early decision-making.

260 Regarding biomarker discovery, proteomics proved to be an important source of information.
261 However, in the classical approaches the plasma samples are subjected to depletion of abundant
262 proteins (Ludwig and Hummon, 2017) and fractionation to identify individual biomarkers (Hayashi
263 et al., 2019; Harberts et al., 2020) which requires more analysis time, specific equipment and higher
264 costs. These constraints led us to explore a top-down strategy that could overcome these difficulties.
265 Thus, having in mind that we aimed to design a readily transferrable method, our approach was
266 meant to be as simple as possible and unlabeled whole plasma were directly read by MALDI-TOF-
267 MS.

268 Our results showed that the performance of the test with whole plasma and standard acquisition
269 settings used in routine microbiological biotyping were excellent in terms of discriminatory power.
270 First, an ensemble between supervised and unsupervised algorithms allowed the overall
271 discrimination of plasma samples corresponding to the three experimental groups. These results
272 showed that each phase comprise a distinctive MALDI-TOF-MS pattern, which turns this approach
273 into a promising tool to determine different phases in sepsis. A recent study reported a top-down
274 plasma analysis showing that differences between samples from healthy donors and cancer patients
275 could be appreciated without the depletion of large abundant proteins by setting a cut-off at 30KDa
276 (Cheon et al., 2016), supporting our results.

277 Furthermore, the performance of our ML algorithms challenged with the test dataset, was able to
278 identify basal, pro-inflammatory and anti-inflammatory/immunosuppressive phases in a very
279 satisfactory way, exceeding 90% of accuracy in some of the tested conditions. The cross validation
280 strategy used herein allows a fine-tuning of the models according to particular needs. Thus,
281 depending on the clinical and epidemiological settings, algorithms with higher sensitivity and lower
282 computational demand like our 5-peaks BDA model could be preferred over those with a good
283 overall accuracy.

284 The peaks found in the 2-20KDa range mostly correspond to small peptides. Plasma peptidome has
285 been proposed as an interesting source of information for diagnostic purposes (Cheon et al., 2016;
286 Dufresne et al., 2018). These peptides are presumably fragments of larger proteins derived from
287 digestion by proteases or non-enzymatic degradation (Greening and Simpson, 2017) but the lack of
288 comprehensive digestome/degradome databases is still a limitation to their study (Shen et al., 2010).
289 Nevertheless, recent reports demonstrate the importance of plasma peptidome as a useful tool for
290 clinical monitoring in septic shock (Aletti et al., 2016; Bauza-Martinez et al., 2018). Although the
291 identification of individual peaks is beyond the objectives of this study, it would be interesting to
292 evaluate them in the future with specific methods with higher resolving power.

293 A major limitation of this study is related to the animal models chosen. Although LPS-induced
294 inflammation/immunosuppression models are widely used, they do not accurately represent the
295 dynamic physiological changes that occur in sepsis (Lewis et al., 2016). Endotoxin challenge
296 promotes a faster and transient release of pro/anti-inflammatory mediators compared to the septic

297 processes. However, these models allowed us to define two discrete phases that actually occur in a
298 septic process. For this reason, we considered this was the most appropriate approach to test the
299 potential of MALDI-TOF-MS analysis in the proof-of concept phase. We are currently validating our
300 results in a dynamic model of sepsis, the cecal ligation and puncture model, with very encouraging
301 results.

302 Our approach has numerous advantages. MALDI-TOF-MS is a simple and speedy method, a critical
303 feature considering the dynamism of sepsis, which is spreading in the clinical setting even in
304 resource-constrained regions. In addition, we used an accessible sample as plasma, without complex
305 pre-processing steps. Finally, we performed our ML analysis in the open source software R that also
306 guarantees the transferability of the bioinformatics tool.

307 In conclusion, our results indicate that plasma peptidome analysis by MALDI-TOF-MS has the
308 potential to be a highly relevant strategy for sepsis patient stratification that could constitute a
309 powerful tool for therapeutic decision making in sepsis depending on the pro- or anti-inflammatory
310 phases the patient is undergoing.

311

312 **5 Conflict of Interest**

313 The authors declare that the research was conducted in the absence of any commercial or financial
314 relationships that could be construed as a potential conflict of interest.

315 **6 Author Contributions**

316 ML designed and performed the bioinformatic analysis. BR and NY conceived and designed the
317 study. MFT, LM and BR performed the experiments with mice and analyzed data. MP and CV
318 provided materials and technical support. MG and BL provided materials and collaborated in study
319 design. ML and NY performed data curation. NY and BR analyzed and discussed the results. BR was
320 responsible for funding acquisition and study supervision. Manuscript was written by NY and BR,
321 and was corrected by ML and BL. All the authors revised and approved the final version of the
322 manuscript.

323 **7 Funding**

324 This study was supported by the Agencia Nacional de Promoción Científica y Tecnológica [grant
325 number PICT 2015-0412], Buenos Aires, Argentina.

326 **8 Acknowledgments**

327 We thank Dr. Martín Isturiz for his eternal accompaniment and support for the development of this
328 study. His outstanding contribution stems from his singular thoughts. Forever in our hearts, Dr.
329 Isturiz. We also thank Dr. Viviana Ritacco for her thoughtful comments on the manuscript. A
330 preliminary version of the manuscript was deposited in the preprint server BioRXiv (doi:
331 10.1101/2020.12.29.424724).

332 **9 Data Availability Statement**

333 The MS datasets generated for this study as well as the analysis pipelines can be found in GitHub
334 [<https://github.com/MarManLed/SepsisData>].

335 10 References

- 336 Al Jalbout, N., Troncoso, R., Jr., Evans, J.D., Rothman, R.E., and Hinson, J.S. (2019). Biomarkers
337 and Molecular Diagnostics for Early Detection and Targeted Management of Sepsis and
338 Septic Shock in the Emergency Department. *J Appl Lab Med* 3, 724-729.
339 doi:10.1373/jalm.2018.027425
- 340 Azevedo, L.C.P., Cavalcanti, A.B., Lisboa, T., Pizzol, F.D., and Machado, F.R. (2018). Sepsis is an
341 important healthcare burden in Latin America: a call to action! *Rev Bras Ter Intensiva* 30,
342 402-404. doi:10.5935/0103-507X.20180061
- 343 Córdoba-Moreno, M.O., Todero, M.F., Fontanals, A., Pineda, G., Daniela, M., Yokobori, N., Ramos,
344 M.V., Barrientos, G., Toblli, J.E., Isturiz, M.A., and Rearte, B. (2019). Consequences of the
345 Lack of IL-10 in Different Endotoxin Effects and its Relationship With Glucocorticoids.
346 *Shock* 52, 264-273. doi:10.1097/SHK.0000000000001233
- 347 Cheon, D.H., Nam, E.J., Park, K.H., Woo, S.J., Lee, H.J., Kim, H.C., Yang, E.G., Lee, C., and Lee,
348 J.E. (2016). Comprehensive Analysis of Low-Molecular-Weight Human Plasma Proteome
349 Using Top-Down Mass Spectrometry. *J Proteome Res* 15, 229-244.
350 doi:10.1021/acs.jproteome.5b00773
- 351 Dolin, H.H., Papadimos, T.J., Chen, X., and Pan, Z.K. (2019). Characterization of Pathogenic Sepsis
352 Etiologies and Patient Profiles: A Novel Approach to Triage and Treatment. *Microbiol*
353 *Insights* 12, 1178636118825081. doi:10.1177/1178636118825081
- 354 Dufresne, J., Bowden, P., Thavarajah, T., Florentinus-Mefailoski, A., Chen, Z.Z., Tucholska, M.,
355 Norzin, T., Ho, M.T., Phan, M., Mohamed, N., Ravandi, A., Stanton, E., Slutsky, A.S., Dos
356 Santos, C.C., Romaschin, A., Marshall, J.C., Addison, C., Malone, S., Heyland, D., Scheltens,
357 P., Killestein, J., Teunissen, C., Diamandis, E.P., Siu, K.W.M., and Marshall, J.G. (2018).
358 The plasma peptidome. *Clin Proteomics* 15, 39. doi:10.1186/s12014-018-9211-3
- 359 Estenssoro, E., Kanoore Edul, V.S., Loudet, C.I., Osatnik, J., Rios, F.G., Vazquez, D.N., Pozo, M.O.,
360 Lattanzio, B., Palizas, F., Klein, F., Piezny, D., Rubatto Birri, P.N., Tuhay, G., Diaz, A.,
361 Santamaria, A., Zakalik, G., and Dubin, A. (2018). Predictive Validity of Sepsis-3 Definitions
362 and Sepsis Outcomes in Critically Ill Patients: A Cohort Study in 49 ICUs in Argentina. *Crit*
363 *Care Med* 46, 1276-1283. doi:10.1097/CCM.0000000000003208
- 364 Estenssoro, E., Loudet, C.I., Edul, V.S.K., Osatnik, J., Rios, F.G., Vasquez, D.N., Pozo, M.O.,
365 Lattanzio, B., Palizas, F., Klein, F., Piezny, D., Rubatto Birri, P.N., Tuhay, G., Diaz, A.,
366 Santamaria, A., Zakalik, G., and Dubin, A. (2019). Health inequities in the diagnosis and
367 outcome of sepsis in Argentina: a prospective cohort study. *Crit Care* 23, 250.
368 doi:10.1186/s13054-019-2522-6
- 369 Fleischmann, C., Scherag, A., Adhikari, N.K., Hartog, C.S., Tsaganos, T., Schlattmann, P., Angus,
370 D.C., and Reinhart, K. (2016). Assessment of Global Incidence and Mortality of Hospital-
371 treated Sepsis. Current Estimates and Limitations. *Am J Respir Crit Care Med* 193, 259-272.
372 doi:10.1164/rccm.201504-0781OC
- 373 Genga, K.R., Shimada, T., Boyd, J.H., Walley, K.R., and Russell, J.A. (2018). The Understanding
374 and Management of Organism Toxicity in Septic Shock. *J Innate Immun* 10, 502-514.
375 doi:10.1159/000487818

- 376 Gibb, S. (2019). "MALDIquantForeign: Import/Export Routines for MALDIquant. ". 0.12 ed.).
- 377 Gibb, S., and Strimmer, K. (2012). MALDIquant: a versatile R package for the analysis of mass
378 spectrometry data. *Bioinformatics* 28, 2270-2271. doi:10.1093/bioinformatics/bts447
- 379 Gibb, S., Strimmer, K. (2015). binda: Multi-Class Discriminant Analysis using Binary Predictors. R
380 package version 1.0.3. .
- 381 Greening, D.W., and Simpson, R.J. (2017). Characterization of the Low-Molecular-Weight Human
382 Plasma Peptidome. *Methods Mol Biol* 1619, 63-79. doi:10.1007/978-1-4939-7057-5_6
- 383 Gunsolus, I.L., Sweeney, T.E., Liesenfeld, O., and Ledebor, N.A. (2019). Diagnosing and Managing
384 Sepsis by Probing the Host Response to Infection: Advances, Opportunities, and Challenges.
385 *J Clin Microbiol* 57. doi:10.1128/JCM.00425-19
- 386 Harberts, E., Liang, T., Yoon, S.H., Opene, B.N., Mcfarland, M.A., Goodlett, D.R., and Ernst, R.K.
387 (2020). Toll-like Receptor 4-Independent Effects of Lipopolysaccharide Identified Using
388 Longitudinal Serum Proteomics. *J Proteome Res* 19, 1258-1266.
389 doi:10.1021/acs.jproteome.9b00765
- 390 Hayashi, N., Yamaguchi, S., Rodenburg, F., Ying Wong, S., Ujimoto, K., Miki, T., and Iba, T.
391 (2019). Multiple biomarkers of sepsis identified by novel time-lapse proteomics of patient
392 serum. *PLoS One* 14, e0222403. doi:10.1371/journal.pone.0222403
- 393 Hou, T.Y., Chiang-Ni, C., and Teng, S.H. (2019). Current status of MALDI-TOF mass spectrometry
394 in clinical microbiology. *J Food Drug Anal* 27, 404-414. doi:10.1016/j.jfda.2019.01.001
- 395 Kassambara, A., and Mundt, F. (2019). "factoextra: Extract and Visualize the Results of Multivariate
396 Data Analyses". R package version 1.0.6 ed.).
- 397 Landoni, V.I., Chiarella, P., Martire-Greco, D., Schierloh, P., Van-Rooijen, N., Rearte, B., Palermo,
398 M.S., Isturiz, M.A., and Fernandez, G.C. (2012). Tolerance to lipopolysaccharide promotes
399 an enhanced neutrophil extracellular traps formation leading to a more efficient bacterial
400 clearance in mice. *Clin Exp Immunol* 168, 153-163. doi:10.1111/j.1365-2249.2012.04560.x
- 401 Lewis, A.J., Seymour, C.W., and Rosengart, M.R. (2016). Current Murine Models of Sepsis. *Surg*
402 *Infect (Larchmt)* 17, 385-393. doi:10.1089/sur.2016.021
- 403 Liaw, A., and Wiener, M. (2002). Classification and Regression by randomForest. *R News* 2, 18-22.
- 404 López Fernández, H., Reboiro-Jato, M., Pérez Rodríguez, J.A., Fdez-Riverola, F., and Glez-Peña, D.
405 (2016). Implementing effective machine learning-based workflows for the analysis of mass
406 spectrometry data. *Journal of Integrated OMICS* 6. doi:10.5584/jiomics.v6i1.196
- 407 Ludwig, K.R., and Hummon, A.B. (2017). Mass spectrometry for the discovery of biomarkers of
408 sepsis. *Mol Biosyst* 13, 648-664. doi:10.1039/c6mb00656f
- 409 Machado, F.R., Cavalcanti, A.B., Bozza, F.A., Ferreira, E.M., Angotti Carrara, F.S., Sousa, J.L.,
410 Caixeta, N., Salomao, R., Angus, D.C., and Pontes Azevedo, L.C. (2017). The epidemiology
411 of sepsis in Brazilian intensive care units (the Sepsis PREvalence Assessment Database,
412 SPREAD): an observational study. *Lancet Infect Dis* 17, 1180-1189. doi:10.1016/S1473-
413 3099(17)30322-5
- 414 Martire-Greco, D., Landoni, V.I., Chiarella, P., Rodriguez-Rodrigues, N., Schierloh, P., Rearte, B.,
415 Isturiz, M.A., and Fernandez, G.C. (2014). all-trans-retinoic acid improves
416 immunocompetence in a murine model of lipopolysaccharide-induced immunosuppression.
417 *Clin Sci (Lond)* 126, 355-365. doi:10.1042/CS20130236

- 418 Montagna, D.R., Duarte, A., Todero, M.F., Ruggiero, R.A., Isturiz, M., and Rearte, B. (2020). Meta-
419 tyrosine modulates the immune response induced by bacterial endotoxins. *Immunobiology*
420 225, 151856. doi:10.1016/j.imbio.2019.10.005
- 421 National Research Council (U.S.) (2011). *Guide for the care and use of laboratory animals*.
422 Washington, District of Columbia: National Academy Press.
- 423 Novosad, S.A., Sapiano, M.R., Grigg, C., Lake, J., Robyn, M., Dumyati, G., Felsen, C., Blog, D.,
424 Dufort, E., Zansky, S., Wiedeman, K., Avery, L., Dantes, R.B., Jernigan, J.A., Magill, S.S.,
425 Fiore, A., and Epstein, L. (2016). Vital Signs: Epidemiology of Sepsis: Prevalence of Health
426 Care Factors and Opportunities for Prevention. *MMWR Morb Mortal Wkly Rep* 65, 864-869.
427 doi:10.15585/mmwr.mm6533e1
- 428 Opal, Steven m., Scannon, Patrick j., Vincent, J.L., White, M., Carroll, Stephen f., Palardy, John e.,
429 Parejo, Nicolas a., Pribble, John p., and Lemke, Jon h. (1999). Relationship between Plasma
430 Levels of Lipopolysaccharide (LPS) and LPS-Binding Protein in Patients with Severe Sepsis
431 and Septic Shock. *The Journal of Infectious Diseases* 180, 1584-1589. doi:10.1086/315093
- 432 Parlato, M., and Cavaillon, J.M. (2015). Host response biomarkers in the diagnosis of sepsis: a
433 general overview. *Methods Mol Biol* 1237, 149-211. doi:10.1007/978-1-4939-1776-1_15
- 434 Parlato, M., Philippart, F., Rouquette, A., Moucadel, V., Puchois, V., Blein, S., Bedos, J.P., Diehl,
435 J.L., Hamzaoui, O., Annane, D., Journois, D., Ben Boutieb, M., Esteve, L., Fitting, C.,
436 Treluyer, J.M., Pachot, A., Adib-Conquy, M., Cavaillon, J.M., Misset, B., and Captain Study,
437 G. (2018). Circulating biomarkers may be unable to detect infection at the early phase of
438 sepsis in ICU patients: the CAPTAIN prospective multicenter cohort study. *Intensive Care*
439 *Med* 44, 1061-1070. doi:10.1007/s00134-018-5228-3
- 440 Pierrakos, C., and Vincent, J.L. (2010). Sepsis biomarkers: a review. *Crit Care* 14, R15.
441 doi:10.1186/cc8872
- 442 Rearte, B., Landoni, V., Laborde, E., Fernandez, G., and Isturiz, M. (2010a). Differential effects of
443 glucocorticoids in the establishment and maintenance of endotoxin tolerance. *Clin Exp*
444 *Immunol* 159, 208-216. doi:10.1111/j.1365-2249.2009.04052.x
- 445 Rearte, B., Maglioco, A., Balboa, L., Bruzzo, J., Landoni, V.I., Laborde, E.A., Chiarella, P.,
446 Ruggiero, R.A., Fernandez, G.C., and Isturiz, M.A. (2010b). Mifepristone (RU486) restores
447 humoral and T cell-mediated immune response in endotoxin immunosuppressed mice. *Clin*
448 *Exp Immunol* 162, 568-577. doi:10.1111/j.1365-2249.2010.04262.x
- 449 Rearte, B., Maglioco, A., Machuca, D., Greco, D.M., Landoni, V.I., Rodriguez-Rodrigues, N., Meiss,
450 R., Fernandez, G.C., and Isturiz, M.A. (2014). Dehydroepiandrosterone and metyrapone
451 partially restore the adaptive humoral and cellular immune response in endotoxin
452 immunosuppressed mice. *Innate Immun* 20, 585-597. doi:10.1177/1753425913502243
- 453 Rubio, I., Osuchowski, M.F., Shankar-Hari, M., Skirecki, T., Winkler, M.S., Lachmann, G., La
454 Rosee, P., Monneret, G., Venet, F., Bauer, M., Brunkhorst, F.M., Kox, M., Cavaillon, J.M.,
455 Uhle, F., Weigand, M.A., Flohe, S.B., Wiersinga, W.J., Martin-Fernandez, M., Almansa, R.,
456 Martin-Loeches, I., Torres, A., Giamarellos-Bourboulis, E.J., Girardis, M., Cossarizza, A.,
457 Netea, M.G., Van Der Poll, T., Scherag, A., Meisel, C., Schefold, J.C., and Bermejo-Martin,
458 J.F. (2019). Current gaps in sepsis immunology: new opportunities for translational research.
459 *Lancet Infect Dis*. doi:10.1016/S1473-3099(19)30567-5

- 460 Schenz, J., Weigand, M.A., and Uhle, F. (2019). Molecular and biomarker-based diagnostics in early
461 sepsis: current challenges and future perspectives. *Expert Rev Mol Diagn* 19, 1069-1078.
462 doi:10.1080/14737159.2020.1680285
- 463 Shen, Y., Liu, T., Tolić, N., Petritis, B.O., Zhao, R., Moore, R.J., Purvine, S.O., Camp, D.G., and
464 Smith, R.D. (2010). Strategy for Degradomic-Peptidomic Analysis of Human Blood Plasma.
465 *Journal of Proteome Research* 9, 2339-2346. doi:10.1021/pr901083m
- 466 Singer, M., Deutschman, C.S., Seymour, C.W., Shankar-Hari, M., Annane, D., Bauer, M., Bellomo,
467 R., Bernard, G.R., Chiche, J.D., Cooper-Smith, C.M., Hotchkiss, R.S., Levy, M.M., Marshall,
468 J.C., Martin, G.S., Opal, S.M., Rubenfeld, G.D., Van Der Poll, T., Vincent, J.L., and Angus,
469 D.C. (2016). The Third International Consensus Definitions for Sepsis and Septic Shock
470 (Sepsis-3). *JAMA* 315, 801-810. doi:10.1001/jama.2016.0287
- 471 Van Der Poll, T., Van De Veerdonk, F.L., Scicluna, B.P., and Netea, M.G. (2017). The
472 immunopathology of sepsis and potential therapeutic targets. *Nat Rev Immunol* 17, 407-420.
473 doi:10.1038/nri.2017.36
- 474 Van Engelen, T.S.R., Joost Wiersinga, W., and Van Der Poll, T. (2018a). "Pathogenesis of Sepsis,"
475 in *Handbook of Sepsis.*), 31-43.
- 476 Van Engelen, T.S.R., Wiersinga, W.J., Scicluna, B.P., and Van Der Poll, T. (2018b). Biomarkers in
477 Sepsis. *Crit Care Clin* 34, 139-152. doi:10.1016/j.ccc.2017.08.010
- 478 Venet, F., Rimmelé, T., and Monneret, G. (2018). Management of Sepsis-Induced
479 Immunosuppression. *Crit Care Clin* 34, 97-106. doi:10.1016/j.ccc.2017.08.007
- 480 Vincent, J.L., Rello, J., Marshall, J., Silva, E., Anzueto, A., Martin, C.D., Moreno, R., Lipman, J.,
481 Gomersall, C., Sakr, Y., and Reinhart, K. (2009). International study of the prevalence and
482 outcomes of infection in intensive care units. *JAMA* 302, 2323-2329.
483 doi:10.1001/jama.2009.1754

484

485

486

487 **Tables**

488 **Table 1.** Performance of the classification models with the top 5, 10, 15, and 20 peaks.

| Peaks | Algorithm | A (%) | S (%) | E (%) | PPV (%) | NPV (%) |
|--------------|------------------|--------------|--------------|--------------|----------------|----------------|
| 5 | BDA | 90.6 | 95.7 | 80 | 90.9 | 89.8 |
| 10 | BDA | 85.6 | 92 | 72.3 | 87.4 | 81.1 |
| 15 | BDA | 87.6 | 93.9 | 74.5 | 88.5 | 85.4 |
| 20 | BDA | 90.1 | 94.3 | 81.4 | 91.4 | 87.3 |
| 5 | RF | 88.2 | 95.7 | 72.7 | 88 | 88 |
| 10 | RF | 91.2 | 91.3 | 90.9 | 95.5 | 83.3 |
| 15 | RF | 88.2 | 91.3 | 81.8 | 91.3 | 81.8 |
| 20 | RF | 94.1 | 95.7 | 90.9 | 95.7 | 90.9 |

A = accuracy, S = sensitivity, E = specificity, PPV = positive predictive value, and NPV = negative predictive value.

489

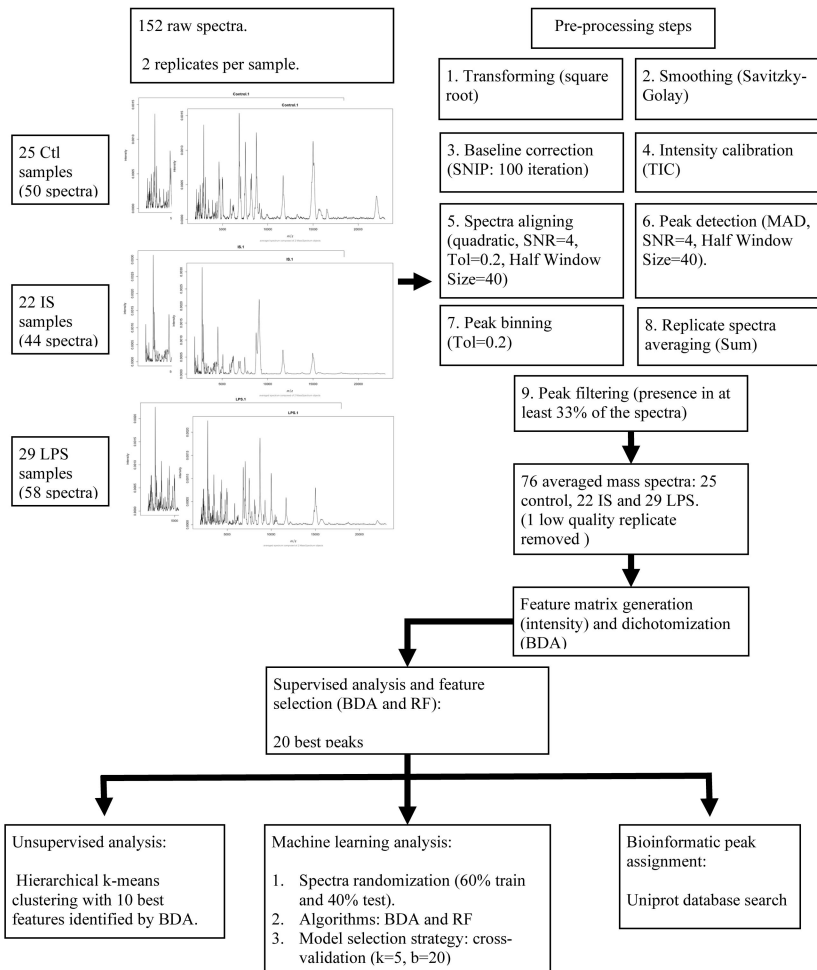
490

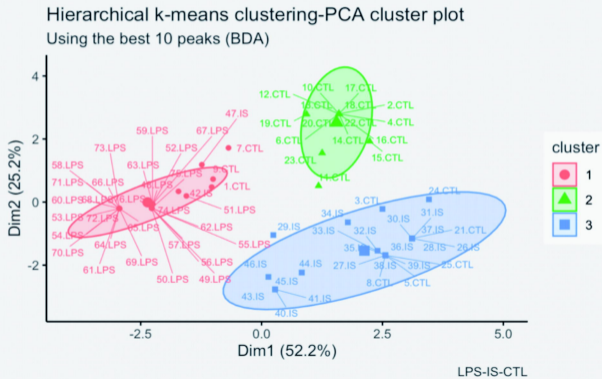
491 **Figure legends**

492 **Figure 1.** MALDI-TOF- MS data analysis pipeline. Abbreviations. CTL: control group; IS:
493 immunosuppression/anti-inflammatory group; LPS: pro-inflammatory group; BDA: binary
494 discriminant analysis; RF: random forest.

495 **Figure 2.** Unsupervised statistical analysis. **(a)** Hierarchical k-means clustering (Hkmc)-Principal
496 Component Analysis (PCA) cluster plot using the top ten peaks selected by the binary discriminant
497 analysis (BDA) algorithm. Labels contain the mice ID and the experimental groups. PC1 (Dim1, x-
498 axis) and 2 (Dim2, y-axis) are depicted. Spectra were clustered into three groups using the Hkmc
499 algorithm, which are represented with three different colors. 95% confidence ellipses were added
500 around cluster means, assuming a multivariate normal distribution. **(b)** Hkmc-PCA cluster
501 composition. The green color represents the CTL mice group, the blue represents the IS group, and
502 the red color represents the LPS group.

503



a**b**